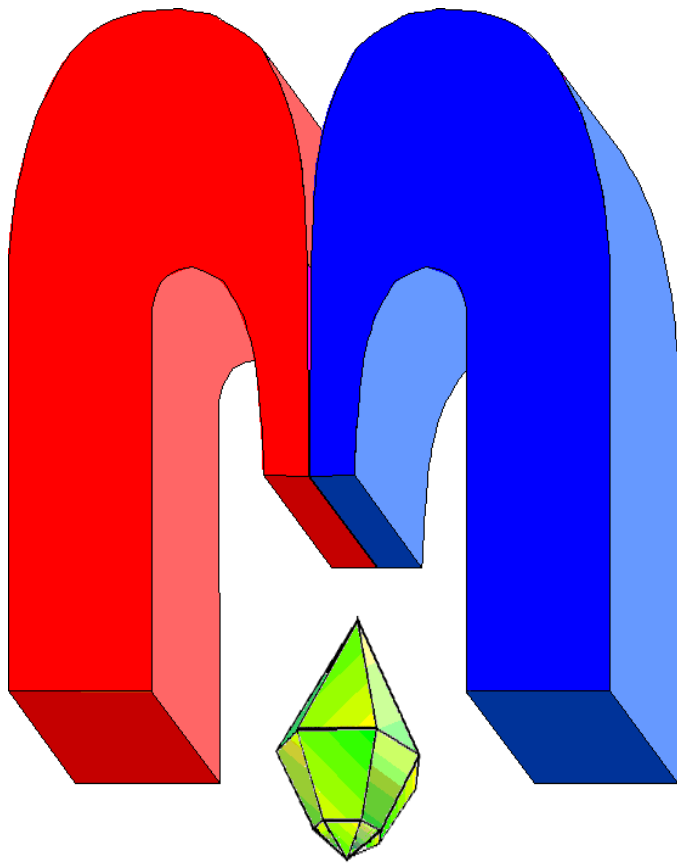


ISSN 2072-5981
doi: 10.26907/mrsej



***magnetic
Resonance
in Solids***

Electronic Journal

Volume 24

Issue 2

Article No 22201

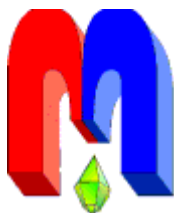
1-6 pages

2022

doi: [10.26907/mrsej-22201](https://doi.org/10.26907/mrsej-22201)

<http://mrsej.kpfu.ru>

<http://mrsej.ksu.ru>



Established and published by Kazan University*
Endorsed by International Society of Magnetic Resonance (ISMAR)
Registered by Russian Federation Committee on Press (#015140),
August 2, 1996
First Issue appeared on July 25, 1997

© Kazan Federal University (KFU)†

"Magnetic Resonance in Solids. Electronic Journal" (MRSej) is a peer-reviewed, all electronic journal, publishing articles which meet the highest standards of scientific quality in the field of basic research of a magnetic resonance in solids and related phenomena.

Indexed and abstracted by
Web of Science (ESCI, Clarivate Analytics, from 2015), Scopus (Elsevier, from 2012), RusIndexSC (eLibrary, from 2006), Google Scholar, DOAJ, ROAD, CyberLeninka (from 2006), SCImago Journal & Country Rank, etc.

Editor-in-Chief

Boris **Kochelaev** (KFU, Kazan)

Honorary Editors

Jean **Jeener** (Universite Libre de Bruxelles, Brussels)

Raymond **Orbach** (University of California, Riverside)

Executive Editor

Yurii **Proshin** (KFU, Kazan)
mrsej@kpfu.ru



This work is licensed under a [Creative Commons Attribution-ShareAlike 4.0 International License](https://creativecommons.org/licenses/by-sa/4.0/).



This is an open access journal which means that all content is freely available without charge to the user or his/her institution. This is in accordance with the [BOAI definition of open access](https://www.boai.ru/).

Technical Editor

Maxim **Avdeev** (KFU, Kazan)

Editors

Vadim **Atsarkin** (Institute of Radio Engineering and Electronics, Moscow)

Yurij **Bunkov** (CNRS, Grenoble)

Mikhail **Eremin** (KFU, Kazan)

David **Fushman** (University of Maryland, College Park)

Hugo **Keller** (University of Zürich, Zürich)

Yoshio **Kitaoka** (Osaka University, Osaka)

Boris **Malkin** (KFU, Kazan)

Alexander **Shengelaya** (Tbilisi State University, Tbilisi)

Jörg **Sichelschmidt** (Max Planck Institute for Chemical Physics of Solids, Dresden)

Haruhiko **Suzuki** (Kanazawa University, Kanazawa)

Murat **Tagirov** (KFU, Kazan)

Dmitrii **Tayurskii** (KFU, Kazan)

Valentine **Zhikharev** (KNRTU, Kazan)

* Address: "Magnetic Resonance in Solids. Electronic Journal", Kazan Federal University; Kremlevskaya str., 18; Kazan 420008, Russia

† In Kazan University the Electron Paramagnetic Resonance (EPR) was discovered by Zavoisky E.K. in 1944.

Magnetic resonance properties of low-dimensional cobalt – Al₂O₃-germanium tunnel contacts[†]

A.V. Kobyakov^{1,2,*}, G.S. Patrin^{1,2}, V.I. Yushkov^{1,2}, Ya.G. Shiyani^{1,2}, R.Yu. Rudenko¹,
N.N. Kosyrev^{2,3}, S.M. Zharkov^{1,2}

¹Siberian Federal University, Krasnoyarsk 660041, Russia

²Kirensky Institute of Physics, Krasnoyarsk Scientific Center, Siberian Branch, Russian Academy of Sciences, Krasnoyarsk 660036, Russia

³Achinsk Branch of Krasnoyarsk State Agrarian University, Achinsk 662100, Russia

*E-mail: nanonauka@mail.ru

(Received July 6, 2022; revised September 30, 2022;
accepted October 2, 2022; published October 12, 2022)

The magnetic resonance properties of a low-dimensional cobalt-Al₂O₃-germanium tunnel contact are studied in this work. The appearance of minima observed at low temperatures on both sides of the cobalt layer was found on the thermomagnetic curve. The value of the temperature minimum differs in magnitude on both sides of the cobalt layer. The position of the minimum in the temperature dependence of magnetization depends on the sample preparation technology. As a result of layer growth, at least two magnetic phases appear. One contribution is from the spins of ferromagnetic particles (cobalt particles with a hexagonal close packed lattice), and additional contributions from the magnetically disordered phase of fine cobalt particles and Co-Al₂O₃ compounds.

PACS: 61.46.-w, 75.70.Cn, 76.50.+g

Keywords: Magnetic resonance, multilayer magnetic films, nanostructures, tunnel effect

1. Introduction

The use of electron tunneling in structures containing semiconductor or dielectric layers, for example, of the ferromagnet/dielectric/semiconductor type, is promising for elements of optoelectronic devices, microwave devices, and other ultrafast microelectronic devices [1,2].

To create high-quality basic elements of spin electronics, it is necessary to solve the problems of creating the spin polarization of electrons, maintaining it for a sufficiently long time, and detecting it. For example, a tunnel junction coupled to a ferromagnetic source of spin-polarized electrons is a candidate for efficient spin injection [3,4]. The injection of spin-polarized electrons in systems of the ferromagnet/dielectric/semiconductor type has a number of features. For example: the interface should not contain the so-called "dead" - disordered layers; defects in the form of layer punctures, roughness from previous layers, etc. [5]. Therefore, controlling the desired magnetic behavior in the synthesis of ferromagnetic complexes such as cobalt [6,7] is still a big problem, and much more work is needed to expand knowledge of the structure-property relationship.

The study of magnetic properties and interfaces in the cobalt/Al₂O₃/germanium system in relation to the technological conditions of synthesis is of considerable interest [8]. Among oxide tunneling barriers, Al₂O₃ shows itself as a high quality atomically thin dielectric. This material exhibits a high barrier height, low tunneling current density, and high breakdown field strength [9].

[†]This paper was selected at the VIII Euro-Asian Symposium "Trends in Magnetism" (EASTMAG-2022), Kazan, August 22–26, 2022. The guest Editor, Prof. R.M. Eremina, was responsible for the publication, which was reviewed according to the standard MRSej procedure.

In this work, we study the magnetic resonance behavior of the $\text{Al}_2\text{O}_3/\text{Ge}/\text{Al}_2\text{O}_3/\text{Co}$ structure with various combinations of deposition rates of magnetic and non-magnetic layers.

2. Experimental details

The $\text{Al}_2\text{O}_3(130\text{ nm})/\text{Ge}(45\text{ nm})/\text{Al}_2\text{O}_3(4.5\text{ nm})/\text{Co}(95\text{ nm})$ structures were obtained by ion-plasma sputtering at a base pressure of $P = 10^{-7}$ Torr in an argon atmosphere with a pressure of 3 mTorr. The substrate material was a cover glass, previously cleaned by ion-plasma etching in the working chamber, immediately before the deposition process. The deposition was carried out on a rotating substrate at its temperature $T \approx 373\text{ K}$. Samples were obtained in two ways (we denote them as A and B) with different combinations of deposition rates of magnetic and nonmagnetic layers.

In set A, all layers were obtained in one cycle. Set B differs in that before the deposition of the magnetic layer, air was admitted into the system to atmospheric pressure in order to saturate the working chamber with gases (as a result of this, the roughness of the next magnetic layer increased, as can be seen from Table 1). Then the pumping was carried out to the base pressure and the last layer of Co was deposited (Table 1).

Table 1. Labeling of samples, velocity, roughness

| | Sample spraying methods. Deposition rate, nm/min | | | | | | | | |
|--|--|------|------|-----|----|------|-----|-----|------|
| | Layers: | A1 | B1 | A2 | B2 | A3 | B3 | A4 | B4 |
| | 1 Al_2O_3 | 0.55 | | | | 0.05 | | | |
| | 2 Ge | 14.4 | | | | 2.4 | | | |
| | 3 Al_2O_3 | 0.55 | | | | 0.05 | | | |
| Average parameters of cobalt surface roughness | 4 Co | 7.2 | | 1.2 | | 1.2 | | 7.2 | |
| | Rms (nm.) | 8.3 | 16.5 | 4 | 12 | 4.4 | 13 | 5.3 | 14.5 |
| | Rz (nm.) | 51.5 | 115 | 36 | 96 | 38 | 106 | 47 | 114 |

The surface morphology of the films was studied using a VeecoMultiMode atomic force microscope. (resolution 1 nm). Table 1 presents the results of measuring the standard deviation of the roughness profile (rms) and the height of irregularities determined by 10 main points (Rz) of the cobalt surface. The morphology, phase, and elemental composition of the films were studied using a JEOL JEM-2100 high-resolution transmission electron microscope equipped with an Oxford Instruments INCA x-sight (EDS) energy-dispersive spectrometer. Magnetic measurements were carried out using the method of the magneto-optical Kerr effect (NanoMOKE-2) and on a SQUID magnetometer. The magnetic field lay in the plane of the film. Before each measurement, the film was first placed in a demagnetizer and then cooled in a zero magnetic field (ZFC mode). As a result, hysteresis loops were obtained for all $\text{Al}_2\text{O}_3/\text{Ge}/\text{Al}_2\text{O}_3/\text{Co}$ samples. To measure the resonance properties, we used a “Bruker E 500 CW EPR”, spectrometer operating at a frequency $f_{MWF} = 9.48\text{ GHz}$.

3. Experimental results and discussion

Analysis of the AFM images (Figure 1 for samples A4) of the cobalt surface observed in the selected area, obtained from all samples, shows that the surface contains the overwhelming amount of cobalt grains with a diameter of 11 nm or more. An analysis of the average intensity profiles of electron diffraction reflections makes it possible to estimate the content of the hcp

and fcc Co phases.

The fraction obtained is approximately 90% hcp-Co and $\approx 10\%$ fcc-Co. There is a feature in all temperature dependences of the saturation magnetization. At low temperatures, a minimum of the saturation magnetization value appears (Figure 2a for samples A3 and A4).

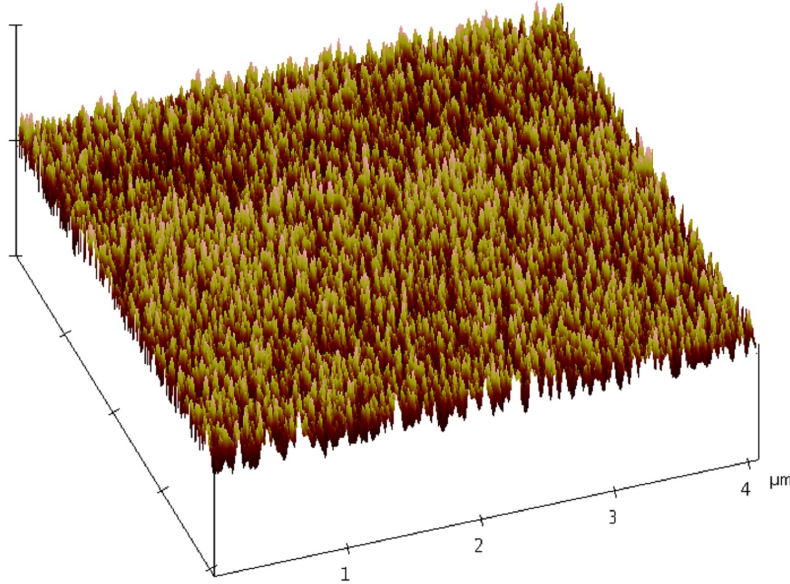


Figure 1. AFM images of cobalt grains on the surface of the $\text{Al}_2\text{O}_3/\text{Ge}/\text{Al}_2\text{O}_3/\text{Co}$ structure for samples A4 (a).

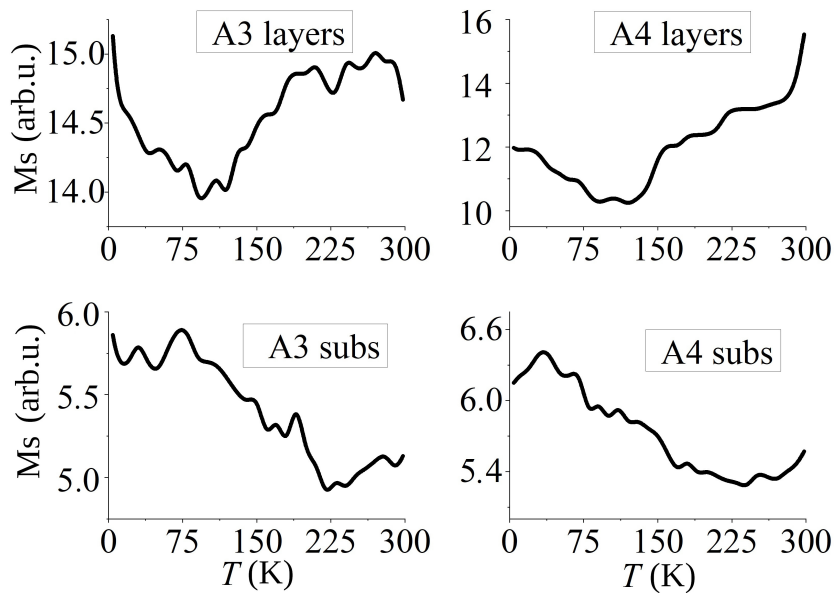


Figure 2. The temperature dependence of saturation magnetization values measured by the Kerr effect method from the side of the layers (A3- and A4 layers) and from the side of the substrate (A3- and A4 subs) of case “A” for structures $\text{Al}_2\text{O}_3/\text{Ge}/\text{Al}_2\text{O}_3/\text{Co}$.

When measuring the ESR response of cobalt for various samples, a spectrum was observed (Figure 3), which for all samples is well approximated by the superposition of two Lorentz-type lines (Figure 3a,b for samples A4 and B4, respectively).

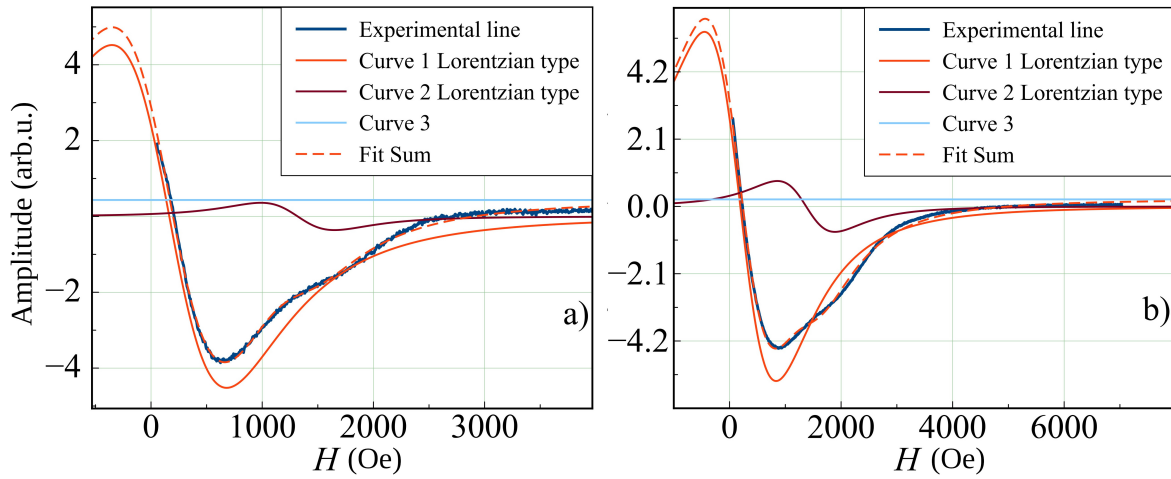


Figure 3. Ferromagnetic resonance spectra of samples A4 (a) and B4 (b) at a temperature of 120 K.

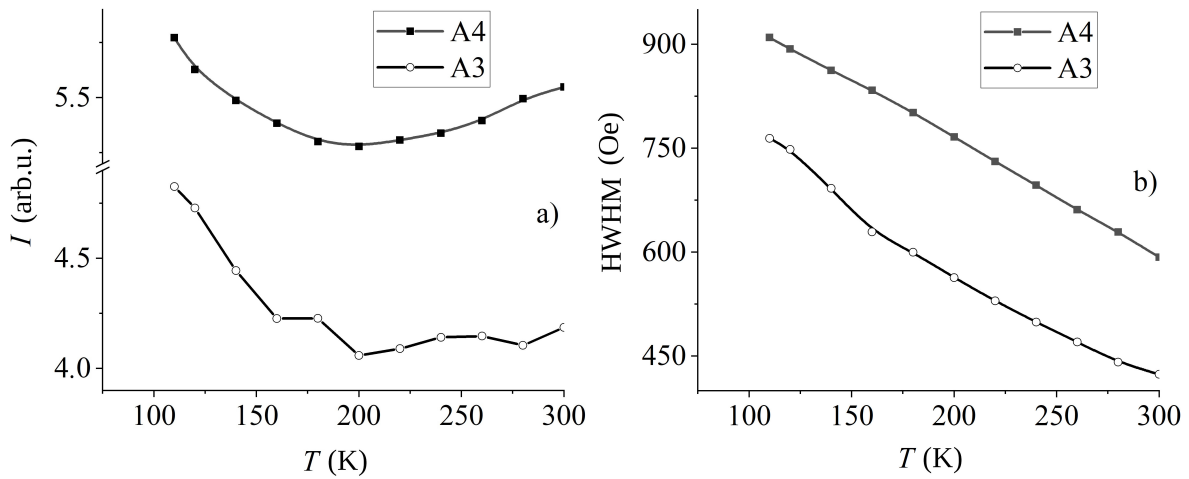


Figure 4. ESR absorption line area (a) and the temperature dependences of the width of Lorentzian line (b) for samples A3 and A4.

Next, the temperature dependences of the sum of the areas under the obtained resonance absorption lines, which are proportional to the number of spins in the sample, were plotted (Fig. 4a for sample A4). The temperature dependences of the width (HWHM) of each Lorentzian line for the ESR spectra are shown in Fig. 4b for samples A4 and A4. On all dependences, there is also a minimum in temperature, slightly shifted upwards, compared with the minimum on the temperature dependences of saturation magnetization. Offset is related to the following. The temperature dependences of the saturation magnetization were taken locally from both sides of the cobalt layer. The temperatures of the minima differ by about 100 K (Fig. 2). The ESR response of cobalt is measured from the entire volume of the sample, and therefore the minimum temperature is averaged in this case.

The observed minimum in the temperature dependences usually indicates the behavior of the magnetization value, as in a spin glass, superparamagnetic or antiferromagnetic layer [10].

The difference in the temperatures of the magnetization minima for case A, on the side of the layers and the substrate, and for case B, shows that the growth of cobalt on the Al_2O_3 oxide layer has a direct effect on the magnetically disordered phase both at the interface and in the volume of cobalt.

Therefore, we can conclude that the reason for the formation of additional magnetic phases is the direct effect of the Al_2O_3 layer on the interface with cobalt, and the effect on the structural growth of the bulk cobalt layer. Among the possible reasons for the formation of an additional magnetic phase, the following can be noted:

1. Cobalt particles can diffuse into the Al_2O_3 layer and a weakly magnetic interface can be formed.
2. $\text{Co-Al}_2\text{O}_3$ granules can form at the interface and in the volume of the cobalt layer. Granules, depending on the concentration of cobalt, can be both superparamagnetic and ferromagnetic. On the temperature dependence of magnetization in the $\text{Co}_{36}\text{Al}_{22}\text{O}_{42}$ structure there is a “freezing” or blocking temperature at $T = 50$ K. The blocking temperature for $\text{Co}_{52}\text{Al}_{20}\text{O}_{28}$ and $\text{Co}_{66}\text{Al}_{13}\text{O}_{21}$ structures is at $T = 150$ and $T = 160$ K, respectively. The values of these temperatures correlate with our experimental data [11, 12].
3. The structure of the grown Al_2O_3 layer affects the structure of the cobalt layer. As a consequence, shape anisotropy or crystallographic magnetic anisotropy of ferromagnetic particles dominates in the cobalt layer.
4. In addition, the magnetically disordered phase of finely dispersed cobalt particles is an additional superparamagnetic phase. This phase is present on both sides of cobalt and in its volume. The presence of such particles was detected on the surface of cobalt.

Then, as a result of the growth of the cobalt layer, at least two magnetic phases appear. One contribution is made by the spins of ferromagnetic particles (cobalt grains hcp), and the other is by additional phases of finely dispersed cobalt particles and $\text{Co-Al}_2\text{O}_3$ compounds present as superparamagnetic grains in the cobalt layer. The competition of magnetic phases at low temperatures leads to the appearance of minima in the saturation magnetization. Magnetic disorder also causes a decrease in saturation magnetization. At low temperatures, these regions are spin-correlated. As the temperature increases, the magnetic field continues to hold spin-correlated regions, while ferromagnetic particles have a predominant effect on the magnetization of the system.

4. Summary

It has been established that a decrease in the rate of deposition of non-magnetic layers, as well as a decrease in the rate of deposition of cobalt in the $\text{Al}_2\text{O}_3/\text{Ge}/\text{Al}_2\text{O}_3/\text{Co}$ system, leads to a decrease in the roughness and the magnitude of the coercive force of cobalt deposited on non-magnetic layers.

It was found that on the surface of cobalt, for all samples, there are granules with a size of 11 nm, which is comparable to the superparamagnetic critical size for cobalt nanoparticles.

The appearance of minima observed at low temperatures on both sides of the cobalt layer was found on the thermomagnetic curve. Measured cobalt ESR response correlates with magnetic measurements. The value of the temperature minimum differs in magnitude on both sides of the cobalt layer. At the temperatures of these minima, an increase in the spread of saturation magnetization between adjacent local areas is noticeable on the spatial map. The facts indicate the existence of at least two magnetic phases in the cobalt layer. By selecting the substrate temperature and deposition rate, one can control the roughness parameters of ferromagnetic films and the presence of fine particles, thereby influencing the value of H_c and ΔH , which makes it possible to optimize functional devices based on them.

Acknowledgments

The work was carried out in the process of fulfilling the state task of the Ministry of Science and Higher Education of the Russian Federation No. FSRZ-2020-0011 “Synthesis and physical foundations of nanoscale film and granular composite materials for spintronics devices”.

References

1. Wilt J., Gong Y., Gong M., Su F., Xu H., Sakidja R., Elliot A., Lu R., Zhao S., Han S., Wu J., *Phys. Rev. Applied* **7**, 064022 (2017)
2. Yamada M., Kuroda F., Tsukahara M., Yamada S., Fukushima T., Sawano K., Oguchi T., Hamaya K., *NPG Asia Materials* **12**, 47 (2020)
3. Fert A., Jaffres H., *Phys. Rev. B* **64**, 184420 (2001)
4. Nikitchenko A.I., Pertsev N.A., *Phys. Rev. Applied* **14**, 034022 (2020)
5. Viglin N.A., Gribov I.V., Tselikhovskaya V.M., Patrakov E.I., *Semiconductors* **53**, 264 (2019)
6. Kahnouji H., Kratzer P., Hashemifar J., *Physical Review B* **99**, 035418 (2019)
7. Rastikian J., Suffit S., Barraud C., Bellec A., Repain V., Roussigne Y., Belmeguenai M., Farhat S., Le Laurent L., Barreteau C., Cherif S. M., *Phys. Rev. Materials* **5**, 014004 (2021)
8. Petrarca A.C., Poma A.M., Giulia V., Bernardini G., *Nanotechnology Reviews* **9**(1), 1538 (2020)
9. Ma P., Guo W., Sun J., Gao J., Zhang G., Xin Q., Li Y., Song A., *Semiconductor Science and Technology* **34**, 10 (2019)
10. Dzhumaliev A. S., Nikulin Y. V. Filimonov Y. A., *Technical Physics* **63**, 1678 (2018)
11. Nakamura S., Iwashita T., Nojima T., Yoshihara A., Ohnuma S., Fujimori H., *Journal of Physics: Conference Series* **200**, 012141 (2010)
12. Nakamura S., Iwashita T., Nojima T., Yoshihara A., Ohnuma S., Fujimori H., *Journal of Physics: Conference Series* **266**, 012019 (2011)